Atmos. Meas. Tech. Discuss., https://doi.org/10.5194/amt-2017-330
Manuscript under review for journal Atmos. Meas. Tech.
Discussion started: 27 October 2017


Atmospheric Measurement Techniques
Open Access
Discussions

# A novel method for calculating ambient aerosol liquid water contents based on measurements of a humidified nephelometer system

**Ye Kuang[1,2], ChunSheng Zhao[1], Gang Zhao[1], JiangChuan Tao[1,2], Nan Ma[2], YuXuan Bian[3]**

[1]{Department of Atmospheric and Oceanic Sciences, School of Physics, Peking University, Beijing, China}

[2]{Institute for Environmental and Climate Research, Jinan University, Guangzhou 511443, China}

[3]{State Key Laboratory of Severe Weather, Chinese Academy of Meteorological Sciences}

Correspondence to: C. S. Zhao (zcs@pku.edu.cn)

**Abstract**

Water condensed on ambient aerosol particles plays significant roles in atmospheric environment, atmospheric chemistry and climate. So far, no instruments are available for real-time monitoring of ambient aerosol liquid water contents (ALWC). In this paper, a novel method is proposed to calculate ambient ALWC based on measurements of a three-wavelength humidified

Atmos. Meas. Tech. Discuss., https://doi.org/10.5194/amt-2017-330
Manuscript under review for journal Atmos. Meas. Tech.
Discussion started: 27 October 2017




nephelometer system. A humidified nephelometer system measures aerosol light scattering coefficients and backscattering coefficients at three wavelengths under dry and different relative humidity (RH) conditions, and therefore provides measurements of light scattering enhancement factor $f(\mathrm{RH})$. The proposed method of calculating ALWC includes two steps. The first step is estimating total volume concentration of ambient aerosol particles in dry state ($V_a(\mathrm{dry})$) with a machine learning method based on measurements of the "dry" nephelometer. The estimated $V_a(\mathrm{dry})$ agrees well with the measured $V_a(\mathrm{dry})$. The second step is estimating the volume growth factor $\mathrm{Vg(RH)}$ of ambient aerosol particles due to water uptake using $f(\mathrm{RH})$ and Ångström exponent. The ALWC is calculated from the estimated $V_a(\mathrm{dry})$ and $\mathrm{Vg(RH)}$. Uncertainty analysis of the estimated $V_a(\mathrm{dry})$ and $\mathrm{Vg(RH)}$ is conducted. This research have bridged the gap between $f(\mathrm{RH})$ and $\mathrm{Vg(RH)}$. The advantage of this new method is that the ambient ALWC can be obtained using only measurements from a three-wavelength humidified nephelometer system. This method will facilitate the real-time monitoring of the ambient ALWC and help for studying roles of aerosol liquid water in atmospheric chemistry, secondary aerosol formation and climate change.

## 1. Introduction

Atmospheric aerosol particles play significant roles in atmospheric environment, climate, human health and the hydrological cycle, and have received much attention in recent decades. One of the most important constituents of ambient atmospheric aerosol is liquid water. The content of condensed water on ambient aerosol particles depends mostly on both aerosol hygroscopicity and ambient relative humidity (RH). Results of previous studies demonstrate that liquid water contributes greatly to the total mass of ambient aerosol particles when the ambient

Atmos. Meas. Tech. Discuss., https://doi.org/10.5194/amt-2017-330
Manuscript under review for journal Atmos. Meas. Tech.
Discussion started: 27 October 2017

Atmospheric Measurement Techniques Discussions

RH is higher than 60% (Bian et al., 2014). And aerosol liquid water has large impacts on aerosol optical properties and aerosol radiative effects (Tao et al., 2014;Kuang et al., 2016). Condensed liquid water on aerosol particles can also serve as a site for multiphase reactions which perturb local chemistry and also further influence the aging processes of aerosol particles (Martin, 2000). Recent studies have shown that aerosol liquid water serves as a reactor which help for efficiently transforming sulfur dioxide to sulfate during haze events and plays crucial roles in worsening atmospheric environment on the North China Plain (NCP) (Wang et al., 2016;Cheng et al., 2016). Hence, the real-time monitoring of ambient aerosol liquid water content (ALWC) is of crucial importance to gain more insights into the roles of aerosol liquid water in atmospheric chemistry, aerosol aging processes and aerosol optical properties.

Few techniques are available for measuring ALWC. The humidified tandem differential mobility analyser systems (HTDMAs) are useful tools and widely used to measure hygroscopic growth factors of ambient aerosol particles (Rader and McMurry, 1986;Wu et al., 2016;Meier et al., 2009). Hygroscopicity parameters retrieved from measurements of HTDMAs can be used to calculate volumes of liquid water. Nevertheless, HTDMAs can not be used to measure the total aerosol water volume because they are not capable of measuring the hygroscopic properties of the entire aerosol size distribution. With size distributions of aerosol particles in their ambient state and dry state, the aerosol water volume can de estimated. Engelhart et al. (2011) deployed a Dry-Ambient Aerosol Size Spectrometer to measure the aerosol liquid water content and volume growth factor of fine particulate matter. This system provides only aerosol water content of aerosol particles within certain size range ( particle diameter less than 500 nm for setup of Engelhart et al. (2011)). In addition, in conjunction with aerosol thermodynamic equilibrium models, ALWC can also be estimated with detailed aerosol chemical information. However, simulations of aerosol hygroscopicity and phase state by using thermodynamic equilibrium models are still very complicated even under the thermodynamic equilibrium hypothesis and these models may cause large bias when used for estimating ALWC (Bian et al., 2014).

A humidified nephelometer system which measures aerosol light scattering coefficient ($\sigma_{sp}$) under dry and different RH conditions is a relatively early method proposed for studying aerosol hygroscopicity (Covert et al., 1972). It provides information about aerosol light scattering enhancement factor $f(\mathrm{RH})$. One advantage of this method is that it has a fast response time and thus measurements can be made continuously which facilitates the monitoring of changing ambient conditions. Another advantage of this method is that it provides information about the overall aerosol hygroscopicity of the entire aerosol size distribution. Both measured $\sigma_{sp}$ of aerosol particles in dry state and $f(\mathrm{RH})$ vary strongly with parameters of particle number size distribution (PNSD), it is difficult to directly link them with volume of aerosol particles in dry state ($V_a(\mathrm{dry})$) and the volume growth factor Vg(RH) of the entire aerosol population. So far, the ALWC can not be directly estimated with measurements from only a humidified nephelometer system. Several studies have shown that if PNSDs in dry state are measured, then an iterative algorithm with Mie theory can be used to calculate an overall aerosol hygroscopic growth factor $\mathrm{g(RH)}$ based on measurements of $f(\mathrm{RH})$ (Zieger et al., 2010;Fierz-Schmidhauser et al., 2010). In this iterative algorithm, the $\mathrm{g(RH)}$ is assumed to be independent of the aerosol diameter. Then ALWC at different RH points can be calculated based on derived $\mathrm{g(RH)}$ and the measured PNSD. This method not only requires additional measurements about PNSD, but also may result in significant deviations of the estimated ALWC because that $\mathrm{g(RH)}$ should be a function of aerosol diameter rather than a constant value. In this paper, we proposed a novel method to calculate the ALWC based only on measurements of a humidified nephelometer system.

## 2. Materials and methods

### 2.1 Datasets

Datasets from five field campaigns are used in this paper. Details about these field campaigns (campaigns F1 to F5, see Table S1) are introduced in the supplemental material. During these field campaigns, sampled aerosol particles have aerodynamic diameters less than 10 µm (by passing through an impactor). The PNSDs in dry state which range from 3nm to 10µm were jointly measured by a Twin Differential Mobility Particle Sizer (TDMPS, Leibniz-Institute for Tropospheric Research , Germany; Birmili et al. (1999)) or a scanning mobility particle size spectrometer (SMPS) and an Aerodynamic Particle Sizer (APS, TSI Inc., Model 3321) with a temporal resolution of 10 minutes.. The mass concentrations of black carbon (BC) were measured using a Multi-Angle Absorption Photometer (MAAP Model 5012, Thermo, Inc., Waltham, MA USA) with a temporal resolution of 1 minute. The aerosol light scattering coefficients ($\sigma_{sp}$) at three wavelengths (450 nm, 550 nm, and 700 nm) were measured using a TSI 3563 nephelometer (Anderson and Ogren, 1998).

Datasets about PNSD, BC and $\sigma_{sp}$ from campaigns F1 to F4 are referred to as D1. Datasets about PNSD, BC and $\sigma_{sp}$ from campaigns F2, F4 and F5 are referred to as D2. Measurements of PNSD and measurements from the humidified nephelometer system during campaign F5 (Wangdu campaign) are used to verify the proposed method of estimating $V_a$(dry) and calculate the ambient ALWC. Details about the humidified nephelometer system during Wangdu campaign are introduced in the supplemental material.

### 2.2 Mie theory

Atmos. Meas. Tech. Discuss., https://doi.org/10.5194/amt-2017-330
Manuscript under review for journal Atmos. Meas. Tech.
Discussion started: 27 October 2017

Atmospheric Measurement Techniques Discussions

The first goal of this research is estimating $V_a(\mathrm{dry})$ from $\sigma_{sp}$ measurements. The $V_a(\mathrm{dry})$ can be integrated from measured PNSD. Thus, datasets of $\sigma_{sp}$ and PNSD are needed to investigate relationships between $\sigma_{sp}$ and $V_a(\mathrm{dry})$. To make sure the data quality of used datasets of $\sigma_{sp}$ and PNSD, the closure between measured $\sigma_{sp}$ and $\sigma_{sp}$ calculated based on measured PNSD and BC with Mie theory (Bohren and Huffman, 2008) is first investigated. Measured $\sigma_{sp}$ has problems regarding angular truncation errors and nonideality of light source. In order to make sure the consistency between measured and modelled $\sigma_{sp}$, modelled $\sigma_{sp}$ are calculated according to practical angular situations of the nephelometer (Anderson et al., 1996). Moreover, during processes of modelling $\sigma_{sp}$, BC is considered to be half externally and half coreshell mixed with other aerosol components, and the mass size distribution of BC used in Ma et al. (2012) which was observed on the NCP is used in this research to account for the mass distributions of BC at different particle sizes. The used refractive index and density of BC are $1.80 - 0.54\mathrm{i}$ and 1.5g $cm^{-3}$ (Kuang et al., 2015). Used refractive index of non light-absorbing aerosol components (other than BC) is$1.53 - 10^{-7}i$ (Wex et al., 2002). Calculation details based on the Mie theory please refer to Kuang et al. (2015). Datasets about PNSD and $\sigma_{sp}$ from D1 are used to perform the closure investigation. Finally, during processes of investigating relationships between $\sigma_{sp}$ and $V_a(\mathrm{dry})$, data points in D1 with relative differences between measured $\sigma_{sp}$ at 550 nm and modelled $\sigma_{sp}$ at 550 nm greater than 10% are excluded. 10% is chosen because of that measured PNSD has uncertainty of larger than 10% (Wiedensohler et al., 2012), and measured $\sigma_{sp}$ has uncertainty of about 9%, this threshold can make sure that most used data points are measured when instruments operated well. .

### 2.3 κ-Köhler theory(Wiedensohler et al., 2012)

Atmos. Meas. Tech. Discuss., https://doi.org/10.5194/amt-2017-330
Manuscript under review for journal Atmos. Meas. Tech.
Discussion started: 27 October 2017


Atmospheric Measurement Techniques Discussions
Open Access
EGU

To simulate the relationships between $f(\mathrm{RH})$ and $\mathrm{Vg(RH)}$, κ-K$\ddot{o}$hler theory is used to describe the hygroscopic growth of aerosol particles with different sizes, and the formula expression of κ-K$\ddot{o}$hler theory can be written as follows (Petters and Kreidenweis, 2007):

$$\mathrm{RH} = \frac{D^3 - {D_d}^3}{D^3 - {D_d}^3(1-\kappa)} \cdot \exp\left(\frac{4\sigma_{s/a} \cdot M_{water}}{R \cdot T \cdot D_p \cdot g \cdot \rho_w}\right) \quad (1)$$

where D is the diameter of the droplet, $D_d$ is the dry diameter, $\sigma_{s/a}$ is the surface tension of solution/air interface, T is the temperature, $M_{water}$ is the molecular weight of water, R is the universal gas constant, $\rho_w$ is the density of water, and $\kappa$ is the hygroscopicity parameter. By combining the Mie theory and the κ-K$\ddot{o}$hler theory, both $f(\mathrm{RH})$ and $\mathrm{Vg(RH)}$ can be simulated. In the processes of calculations for modelling $f(\mathrm{RH})$ and $\mathrm{Vg(RH)}$, the treatment of BC is same with those introduced in Sect.2.2. As aerosol particle grow due to aerosol water uptake, the refractive index will change. In the Mie calculation, impacts of aerosol liquid water on the refractive index are considered on the basis of volume mixing rule. The used refractive index of liquid water is $1.33 - 10^{-7}i$ (Seinfeld and Pandis, 2006).

### 2.4 Parameterization scheme for $f(\mathrm{RH})$

The $f(\mathrm{RH})$ is defined as $f(\mathrm{RH}) = \sigma_{sp}(RH, 550\ nm)/\sigma_{sp}(dry, 550\ nm)$ where $\sigma_{sp}(RH, 550\ nm)$ and $\sigma_{sp}(dry, 550\ nm)$ represents $\sigma_{sp}$ at wavelength 550 nm under certain RH and dry conditions. Additionaly, $\mathrm{Vg(RH)}$ is defined as $\mathrm{Vg(RH)} = V_a(\mathrm{RH})/V_a(\mathrm{dry})$, where $V_a(\mathrm{RH})$ represents total volume of aerosol particles under certain RH conditions.

A physically based single-parameter representation is proposed by Brock et al. (2016) to describe $f(\mathrm{RH})$. The parameterization scheme is written as:

Atmos. Meas. Tech. Discuss., https://doi.org/10.5194/amt-2017-330
Manuscript under review for journal Atmos. Meas. Tech.
Discussion started: 27 October 2017


Atmospheric Measurement Techniques Discussions

$$f(\mathrm{RH}) = 1 + \kappa_{sca}\frac{RH}{100-RH} \quad (2)$$

where $\kappa_{sca}$ is the parameter which fits $f(\mathrm{RH})$ best. Here, a brief introduction is given about the physical understanding of this parameterization scheme. For aerosol particles whose diameters larger than 100 nm, regardless of the kelvin effect, the hygroscopic growth factor for a aerosol particle can be approximately expressed as the following (Brock et al., 2016): $\mathrm{g(RH)} \cong (1 + \kappa\frac{RH}{100-RH})^{1/3}$. Enhancement factor in volume can be expressed as the cube of g(RH). Of particular note is that aerosol particles larger than 100 nm contribute the most to $\sigma_{sp}$ and $V_a(\mathrm{dry})$, which means that if κ values of aerosol particles of different sizes are the same, then Vg(RH) can be approximately expressed as $\mathrm{Vg(RH)} = 1 + \kappa\frac{RH}{100-RH}$. In addition, $\sigma_{sp}$ is usually proportional to $V_a(\mathrm{dry})$ which indicates that the relative change in $\sigma_{sp}$ due to aerosol water uptake is roughly proportional to relative change in aerosol volume. Therefore, $f(\mathrm{RH})$ might also be well described by using the formula form of equation (2). Previous studies have shown that this parameterization scheme can describe $f(\mathrm{RH})$ well (Brock et al., 2016;Kuang et al., 2017a).

During processes of measuring $f(\mathrm{RH})$, the sample RH in the "dry" nephelometer ($RH_0$) is not zero. According to equation (2), the measured $f(\mathrm{RH})_{measure} = \frac{f(\mathrm{RH})}{f(RH_0)}$ should be fitted using the following formula:

$$f(\mathrm{RH})_{measure} = (1 + \kappa_{sca}\frac{RH}{100-RH})/(1 + \kappa_{sca}\frac{RH_0}{100-RH_0}) \quad (3)$$

Based on this equation, $\kappa_{sca}$ can be calculated from measured $f(\mathrm{RH})$ directly.

The typical value of $RH_0$ measured in the "dry" nephelometer during Wangdu campaign is about 20%. The importance of the $RH_0$ correction changes under different aerosol hygroscopicity and $RH_0$ conditions. The parameter $\kappa_{sca}$ is fitted with and without consideration of $RH_0$ for $f$(RH) measurements during Wangdu campaign, and the results are shown in Fig.1. The results demonstrate that, overall, the $\kappa_{sca}$ will be underestimated if the influence of $RH_0$ is not considered, and the larger the $\kappa_{sca}$ the more that the $\kappa_{sca}$ will be underestimated.

In addition, based on discussions about the physical understanding of equation (2), the Vg(RH) should be well described by the following equation:

$$\mathrm{Vg(RH)} = 1 + \kappa_{Vf}\frac{RH}{100-RH} \quad (4)$$

where $\kappa_{Vf}$ is the parameter which fits Vg(RH) best.

## 3. Results and discussions

### 3.1 Estimation of $V_a$(dry) from measurements of the "dry" nephelometer

The first step of the proposed method is estimating $V_a$(dry) from measurements of the "dry" nephelometer. The investigation about the relationship between $V_a$(dry) and parameters measured by the "dry" nephelometer is required. Results of previous studies demonstrated that $\sigma_{sp}$ of aerosol particles is roughly proportional to $V_a$(dry) (Pinnick et al., 1980). To confirm this conclusion, datasets of concurrently measured $\sigma_{sp}$ (not corrected for angular truncation error) and PNSD of aerosol particles in dry state from D1 are used to investigate the relationships between measured $\sigma_{sp}$ and $V_a$(dry). The measured $V_a$(dry) is integrated from simultaneously measured PNSD. To gain a first glimpse about the roughly proportional relationship between $\sigma_{sp}$

and $V_a$(dry). All valid data points of measured $\sigma_{sp}$ at 550 nm and $V_a$(dry) are plotted against each other and presented in Fig.2a. The results demonstrate that the $\sigma_{sp}$ is highly correlated with $V_a$(dry), and the square of correlation coefficient between them is 0.92. The roughly proportional relationship exists between $V_a$(dry) and $\sigma_{sp}(550\ nm)$. However, the ratio $\sigma_{sp}(550\ nm)/V_a$(dry) (hereinafter referred to as $R_{Vsp}$) varies significantly. The $R_{Vsp}$ for points in Fig.2a range 1.54 to 6.9 $cm^3/(\mu m^3 \cdot Mm)$, and the average $R_{Vsp}$ is 4.35 $cm^3/(\mu m^3 \cdot Mm)$. If this average $R_{Vsp}$ is used for estimations of $V_a$(dry) based on measured $\sigma_{sp}(550\ nm)$, large bias may occur. Datasets of PNSD and $\sigma_{sp}$ measured by the "dry" nephelometer during Wangdu campaign are used for investigating the performance of using the average $R_{Vsp}$ in Fig.2a for estimating $V_a$(dry), and the results are shown in Fig.2b. The x-axis represents measured $V_a$(dry) which is integrated from measured PNSD. The y-axis represents estimated $V_a$(dry) with an average $R_{Vsp}$. The results demonstrate that although a good correlation exists between estimated $V_a$(dry) and measured $V_a$(dry) (square of correlation coefficient between them is 0.83), large errors might occur, about 30% of data points have relative differences larger than 30%. More sophisticated method which can partially account for the variation of $R_{Vsp}$ is needed for estimating $V_a$(dry) based on measurements of the "dry" nephelometer.

For developing a method which can partially consider the variation of $R_{Vsp}$, factors which determine the variation in $R_{Vsp}$ should be aware of. Here, the quantitative relationship between $V_a$(dry) and $\sigma_{sp}$ is analyzed. The $\sigma_{sp}$ and $V_a$(dry) can be expressed as the following:

$$\sigma_{sp} = \int \pi r^2 Q_{sca}(m,r)\mathrm{n(r)dr} \quad (5)$$

$$V_a(\mathrm{dry}) = \int \frac{4}{3}\pi r^3 \mathrm{n(r)dr} \quad (6)$$

where $Q_{sca}(m,r)$ is scattering efficiency for a particle with refractive index m and particle radius r, n(r) is the aerosol size distribution. As presented in equation (5) and (6), relating $V_a(\text{dry})$ with $\sigma_{sp}$ involves complex relation between $Q_{sca}(m,r)$ and particle diameter, and this relationship can be simulated using Mie theory. In consideration of aerosol refractive index at visible spectral range, aerosol chemical components can be classified into two categories: the light absorbing component and the almost light non-absorbing components (inorganic salts and acids, and most of the organic compounds). Near the visible spectral range, the light absorbing component can be referred to as BC. BC particles are either externally or internally mixed with other aerosol components. In view of this, $Q_{sca}$ at 550 nm as a function of particle diameter for four types of aerosol particles is simulated using Mie theory: almost non-absorbing aerosol particle, BC particle, BC particle core-shell mixed with non-absorbing components and the radius of inner BC core are 25 nm and 100 nm, respectively. Same with those introduced in Sect.2.2, used refractive indices of BC and light non-absorbing components are $1.80 - 0.54\text{i}$ and $1.53 - 10^{-7}\text{i}$ , respectively. The simulated results are shown in Fig.3a. Near the visible spectral range, most of ambient aerosol particles are almost non-absorbing, and their $Q_{sca}$ varies more like the blue line shown in Fig.3a. In the case of the blue line, aerosol particles with diameter less than about 800 nm, their $Q_{sca}$ increases almost monotonously with the particle diameter and can be approximately as a linear function to some extent. Fig.3b shows the simulated size-resolved accumulative contribution to scattering coefficient at 550 nm for all PNSDs measured during Wangdu campaign. The results indicate that for continental aerosol particles without influences of dust, in most cases, all particles with diameter less than about 800 nm contribute more than 80% to total $\sigma_{sp}$. Therefore, for equation (5), If we express $Q_{sca}(m,r)$ as $Q_{sca}(m,r) = \text{k} \cdot \text{r}$, then equation (5) can be expressed as the following:

$$\sigma_{sp} = \mathrm{k} \cdot \int \pi r^3 \mathrm{n(r)dr} \qquad (7)$$

This explains why $\sigma_{sp}(550\ nm)$ is roughly proportional to $V_a(\mathrm{dry})$. However, the value k varies a lot for different particle diameters, which lead to the $R_{Vsp}$ affected greatly by the PNSD which determines weights of influences of aerosol particles with different diameters on $R_{Vsp}$. The difference between the blue line and black line shown in Fig.3a indicates that fraction of externally mixed BC particles in all particles and their sizes will impact on $R_{Vsp}$ largely. The difference between the black line and the red line as well as the difference between the solid red line and the dashed red line shown in Fig.3a indicate that how BC mixed with and how much BC core-shell mixed with other components also exert significant influences on $R_{Vsp}$. In summary, the variation of $R_{Vsp}$ is mainly determined by variations in PNSD, mass size distribution and mixing state of BC. It is difficult to find a simple functional relationship between measured $\sigma_{sp}$ and $V_a(\mathrm{dry})$.

The "dry" nephelometer provides not only one single $\sigma_{sp}$ at 550 nm, it measures six parameters including $\sigma_{sp}$ and back scattering coefficients ($\sigma_{bsp}$) at three wavelengths. The Ångström exponent calculated from spectral dependence of $\sigma_{sp}$ provide information on mean predominant aerosol size and is associated mostly with PNSD. However, the mass size distribution and mixing state of BC also impact on Ångström exponent. The variation of the hemispheric backscattering fraction (HBF) which is the ratio between $\sigma_{bsp}$ and $\sigma_{sp}$, is essentially related with mass size distribution and mixing state of BC if the PNSD is fixed (Ma et al., 2012). If the PNSD and mass size distribution of BC are fixed, higher HBF at 550 nm means that BC particles are more internally (core-shell) mixed with other aerosol components (Ma et al., 2012). Hence, variations in both Ångström exponent and HBF are associated with PNSD, mass size distribution and mixing state of BC. As a result, the Ångström exponent and HBF together might constrain the variation of $R_{Vsp}$ better. In keeping with this philosophy, $R_{Vsp}$ shown in Fig.2a are spread into a two-dimensional gridded plot as shown in Fig.4a. Ångström exponent values are calculated based on concurrently measured $\sigma_{sp}$ at 450 nm and 550 nm from TSI 3563 nephelometer. In Fig.4a, two regions are distinctly differed. In general, when HBF at 550 nm is larger than 0.14 and Ångström exponent is larger than 1, the $R_{Vsp}$ tends to be much smaller. This can be qualitatively understood. For the case of the blue line shown in Fig.3a, if particle diameter is smaller than about 750 nm, overall, the k value is larger if the particle diameter is larger. Smaller Ångström exponent and HBF at 550 nm together correspond to relatively larger particle diameter and therefore larger $R_{Vsp}$. However, more details about the average variation pattern of $R_{Vsp}$ with changes of HBF at 550 nm and Ångström exponent are difficult to be disentangled, due to that influences of PNSD, mass size distribution and mixing state of BC on $R_{Vsp}$ are highly nonlinear. The percentile value of standard deviation of $R_{Vsp}$ values within each grid of Fig.4a divided by their average is shown in Fig.4b. If HBF at 550 nm is less than 0.13, in most cases, percentile values shown in Fig.4b are less than 7%, which means that in this region $R_{Vsp}$ varies little within each grid. However, if HBF at 550 nm is larger than 0.14, in most cases, percentile values shown in Fig.4b are near or even larger than 20%, which means that in this region even HBF and Ångström exponent are fixed, $R_{Vsp}$ still varies a lot. These results imply that if using results shown in Fig.4a as a look up table for estimating $R_{Vsp}$, large bias may occur when HBF at 550 nm is larger than 0.14.

Datasets of $\sigma_{sp}$ and $\sigma_{bsp}$ measured by the "dry" nephelometer and concurrently measured PNSD during Wangdu campaign are used for verifying the performance of using results shown

Atmos. Meas. Tech. Discuss., https://doi.org/10.5194/amt-2017-330
Manuscript under review for journal Atmos. Meas. Tech.
Discussion started: 27 October 2017

Atmospheric Measurement Techniques
Open Access
Discussions

in Fig.4a as a look up for estimating $R_{Vsp}$ and further estimating $V_a(\text{dry})$, and results are shown in Fig.5a. Compared with the results shown in Fig.2b, the look up table method has improved the estimation of $V_a(\text{dry})$ markedly (square of correlation coefficient between measured and estimated $V_a(\text{dry})$ increased from 0.83 to 0.9). It is noticeable that for points with HBF at 550 nm larger than about 0.13, $V_a(\text{dry})$ are systematically underestimated. This result is consistent with the previous analysis that if using results shown in Fig.4a as a look up table for estimating $R_{Vsp}$, large bias may occur when HBF at 550 nm is larger than 0.14.

Six parameters are measured by the "dry" nephelometer, however, only three parameters including $\sigma_{sp}$ at 450 nm and 550 nm, and $\sigma_{bsp}$ at 550 nm are used if using the look up table shown in Fig.4a for estimating $V_a(\text{dry})$. It can be seen from the results shown in Fig.4b, when the HBF at 550 nm is larger than 0.14, variations in $R_{Vsp}$ are poorly constrained. Based on the improvement achieved by using a look up table, we speculate that if all six parameters measured by the "dry" nephelometer are used together, then HBF at three wavelengths and Ångström exponent calculated both from $\sigma_{sp}$ at 450 nm and 550 nm and $\sigma_{sp}$ at 550 nm and 700 nm together can constrain variation in $R_{Vsp}$ better. Machine learning methods which can handle many input parameters are capable of learning from historical datasets and then make predictions are powerful tools for tackling highly nonlinear problems. In the light of this, the idea came out that predicting $V_a(\text{dry})$ based on six optical parameters measured by the "dry" nephelometer might be accomplished by using a machine learning method. In this paper, we choose the machine learning function RidgeCV (ridge regression) from the linear model of module Scikit-learn of computer language Python (Pedregosa et al., 2011) for training the historical datasets of concurrently measured $V_a(\text{dry})$ and six raw parameters measured by the "dry" nephelometer

Atmos. Meas. Tech. Discuss., https://doi.org/10.5194/amt-2017-330
Manuscript under review for journal Atmos. Meas. Tech.
Discussion started: 27 October 2017


from several field campaigns (Corresponding to data points shown in Fig.2a). Measurements during Wangdu campaign again are used for evaluating this machine learning method and the results are shown in Fig.5b. Compared with results shown in Fig.5a, the estimation of $V_a$(dry) is further improved, not only reflected in the increase of square of correlation coefficient, but also reflected in the change of the slope. And almost all points with HBF at 550 nm larger than 0.13 distributed within or near the 20% relative difference line. For the machine learning method, the square of correlation coefficient between measured and estimated $V_a$(dry) is 0.93, with 75% and 43% points have absolute relative differences less than 20% and 10%, respectively. And the standard deviations of absolute and relative differences between measured and estimated $V_a$(dry) are 8.4 $\mu m^3/cm^3$ and 10%, respectively.

Measured PNSDs and values of $\sigma_{sp}$ at 550 nm during Wangdu campaign are shown in Fig.6a and Fig.6b, respectively. The results show that new particle formation phenomena are frequently observed during Wangdu campaign. In addition, both time series of estimated values of $V_a$(dry) using the machine learning method and time series of $V_a$(dry) which are integrated from measured PNSDs are shown in Fig.6c. The results demonstrate that overall, under different pollution levels and during periods with and without new particle formation phenomena, predicted $V_a$(dry) agrees well with measured $V_a$(dry). If a reasonable aerosol density is assumed, measurements from a three-wavelength nephelometer can also be used to estimate total mass concentrations of ambient aerosol particles in dry state.

Machine learning methods do not explicitly express relationships between many variables, however, they learn and implicitly construct complex relationships among variables from historical datasets. Many different and comprehensive machine learning methods are developed for diverse applications, and can be directly used as a tool for solving a lot of nonlinear problems which may not be mathematically well understood. We suggest that using machine learning method for estimating $V_a(\mathrm{dry})$ based on measurements of the "dry" nephelometer. The way of estimating $V_a(\mathrm{dry})$ with machine learning method might be applicable for different regions around the world if used estimators are trained with corresponding regional historical datasets.

### 3.2 Bridge the gap between $f(\mathrm{RH})$ and $\mathrm{Vg}(\mathrm{RH})$

The approximate proportional relationship between $\sigma_{sp}$ and $V_a(\mathrm{dry})$ introduced in Sect.3.1 is only applicable for aerosol particles of constant refractive index, which is not the case for aerosol particles growing by addition of water with increasing RH (Hegg et al., 1993). As aerosol particles grow under conditions of increasing RH, the aerosol scattering efficiency change nonlinearly and can even decrease. It is difficult to use the same method as introduced in Sect.3.1 to estimate the total aerosol volume of aerosol particles in ambient RH conditions. If $\mathrm{Vg}(\mathrm{RH})$ can be directly estimated from measured $f(\mathrm{RH})$, then the ALWC can be estimated. Relating $f(\mathrm{RH})$ to $\mathrm{Vg}(\mathrm{RH})$ involves complicated variations of aerosol scattering efficiency as a function of growing particle diameter due to aerosol water uptake, and this relationship can be described using Mie theory and κ-Köhler theory. As discussed in Sect.2.4, $f(\mathrm{RH})$ and $\mathrm{Vg}(\mathrm{RH})$ can be described by the formula form of equation (2) and (4). To consolidate this conclusion, a simulative experiment is conducted. In the simulative experiment, average PNSD in dry state and mass concentration of BC during the Haze in China (HaChi) campaign (Kuang et al., 2015) are used. During HaChi campaign, size-resolved $\kappa$ distributions are derived from measured size-segregated chemical compositions (Liu et al., 2014) and their average is used in this experiment to account the size dependence of aerosol hygroscopicity. Modelled results of $f(\mathrm{RH})$ and

Vg(RH) are shown in Fig.7. Results demonstrate that modelled $f$(RH) and Vg(RH) can be well parameterized using the formula form of equation (2) and (4). Fitted values of $\kappa_{sca}$ and $\kappa_{Vf}$ are 0.227 and 0.285, respectively. This result indicates that if linkage between $\kappa_{sca}$ and $\kappa_{Vf}$ is established, measurements of $f$(RH) can be directly related to Vg(RH).

Many factors have significant influences on the relationships between $f$(RH) and Vg(RH), such as PNSD, BC mixing state and the size-resolved aerosol hygroscopicity. To gain insights into the relationships between $\kappa_{sca}$ and $\kappa_{Vf}$, a simulative experiment using Mie theory and κ-Köhler theory is designed. In this experiment, all PNSDs at dry state along with mass concentrations of BC from D2 are used, characteristics of these PNSDs can be found in Kuang et al. (2017a). As to size-resolved aerosol hygroscopicity, a number of size-resolved $\kappa$ distributions were derived from measured size-segregated chemical compositions during HaChi campaign (Liu et al., 2014). Their results demonstrate that overall, size-resolved $\kappa$ distributions have three modes: highly hygroscopic mode with diameters of aerosol particles ranging from 150 nm to 1 µm, less hygroscopic mode with diameters of aerosol particles less than 150 nm and nearly hydrophobic mode with diameters of aerosol particles larger than 1 µm. The shape of the average size-resolved $\kappa$ distribution during HaChi campaign (black line shown in Fig.9a) is used in the designed experiment. Other than the shape of size-resolved $\kappa$ distribution, the overall aerosol hygroscopicity which determines the magnitude of $f$(RH) also have large impacts on the relationship between $\kappa_{sca}$ and $\kappa_{Vf}$. In view of this, ratios range from 0.05 to 2 with an interval of 0.05 are multiplied with the aforementioned average size-resolved $\kappa$ distribution (the black line shown in Fig.9a) to produce a number of size-resolved $\kappa$ distributions which represent aerosol particles from nearly hydrophobic to highly hygroscopic. During simulating processes, each

PNSD is modelled with all produced size-resolved $\kappa$ distributions. In the following, the ratio $\kappa_{Vf}/\kappa_{sca}$ termed as $R_{Vf}$ is used to indicate the relationship between $\kappa_{sca}$ and $\kappa_{Vf}$.

In consideration of that values of Ångström exponent contain information about PNSD (Kuang et al., 2017a) and values of $\kappa_{sca}$ represent overall hygroscopicity of ambient aerosol particles, and both the two parameters can be directly calculated from measurements of a three-wavelength humidified nephelometer system (Kuang et al., 2017a). Simulated $R_{Vf}$ values are spread into a two-dimensional gridded plot. The first dimension is Ångström exponent with an interval of 0.02 and the second dimension is $\kappa_{sca}$ with an interval of 0.01. Average $R_{Vf}$ value within each grid is represented by color and shown in Fig.8a. Values of Ångström exponent corresponding to used PNSDs are calculated from simultaneously measured $\sigma_{sp}$ values at 450 nm and 550 nm from TSI 3563 nephelometer. Results shown in Fig.8a exhibit that both PNSD and overall aerosol hygroscopicty have significant influences on $R_{Vf}$. Simulated values of $R_{Vf}$ range from 0.8 to 1.7 with an average of 1.2. Overall, $R_{Vf}$ value is lower when value of Ångström exponent is larger. With respect to influences of $\kappa_{sca}$ on $R_{Vf}$, if Ångström exponent is larger than about 1.1, $\kappa_{sca}$ have small influences on $R_{Vf}$ while its influence is remarkable when Ångström exponent is lower than 1.1. In addition, the percentile value of standard deviation of $R_{Vf}$ values within each grid divided by its average is shown in Fig.8b. In most cases, these percentile values are less than 10% (about 90%) which demonstrates that $R_{Vf}$ varies little within each grid shown in Fig.8a. This implies that results of Fig.8a can serve as a look up table to estimate $R_{Vf}$ and thereby $\kappa_{Vf}$ values can be directly predicted from measurements of a three-wavelength humidified nephelometer system.

For the look up table shown in Fig.8a, a fixed size-resolved $\kappa$ distribution is used, which might not be able to capture variations of $R_{Vf}$ induced by different types of size-resolved $\kappa$ distributions under different PNSD conditions. A simulative experiment is conducted to investigate the performance of this look up table. In this experiment, the following datasets are used: PNSDs and mass concentrations of BC from D2 (the number of used PNSD is 11996), and size-resolved $\kappa$ distributions from HaChi campaign (Liu et al., 2014) which are presented in Fig.9a (the number is 23). Results shown in Fig.9a imply that the shape of size-resolved $\kappa$ distribution has no apparent correlation with pollution degrees and varies a lot. During the simulating processes, for each PNSD, it is used to simulate $R_{Vf}$ values corresponding to all used size-resolved $\kappa$ distributions, therefore, 275908 $R_{Vf}$ values are modelled. Also, modelled values of $\kappa_{sca}$ and corresponding values of modelled Ångström exponent are together used to estimate $R_{Vf}$ values using the look up table shown in Fig.8a. Results of relative differences between estimated and modelled $R_{Vf}$ values under different pollution conditions are shown in Fig.9b. Overall, 88% of points have absolute relative differences less than 15%, and 68% of points have absolute relative differences less than 10%. This look up table performs better when the air is relatively polluted.

### 3.3 Estimation of the ambient ALWC

During the Wangdu campaign, there are ten days of measurements from the humidified nephelometer system are available. Values of $\kappa_{sca}$ are first fitted from observed $f(\mathrm{RH})$ curves and then linearly interpolated to times of ambient RH points (one $f(\mathrm{RH})$ curve lasts about 45 minutes, the time resolution of used ambient RH is five minutes), and the results are shown in Fig.20a. The RH range of one $f(\mathrm{RH})$ cycle is about 50% to 90%. The estimated values of $\kappa_{Vf}$

Atmos. Meas. Tech. Discuss., https://doi.org/10.5194/amt-2017-330
Manuscript under review for journal Atmos. Meas. Tech.
Discussion started: 27 October 2017



using results shown in Fig.20a as a look up table is also shown in Fig.20a. During this observation period, $\kappa_{sca}$ ranges from 0.05 to 0.3 with an average of 0.19. Estimated values of $R_{Vf}$ ranges from 0.86 to 1.47, with an average of 1.15. Estimated values of $\kappa_{Vf}$ ranges from 0.05 to 0.35, with an average of 0.22. Time series of ambient RH is shown in Fig.20b, and RH points with RH larger than 95% are excluded because the measurements of ambient RH at this range is highly uncertain. With estimated values of $\kappa_{Vf}$ and measured ambient RH, Vg(RH) of aerosol particles in ambient RH states can be estimated. Then, with measured $V_a(\text{dry})$ (shown in Fig.20c) which is integrated from measured PNSD, water volumes of ambient aerosol particles are estimated and shown in Fig.20c. During this observation period, estimated water volume of ambient aerosol particles mainly range from 1 to 300 $\mu m^3/cm^3$, with an average of 42 $\mu m^3/cm^3$.

### 3.4 Uncertainty analysis

According to the equation $\text{Vg(RH)} = 1 + \kappa_{Vf}\frac{RH}{100-RH}$, the estimated volume of aerosol liquid water ($V_{water}$) can be expressed as: $V_{water} = V_a(\text{dry}) \cdot \kappa_{sca} \cdot R_{Vf} \cdot \frac{RH}{100-RH}$. Neglecting measurement uncertainty of ambient RH, uncertainties contribute to $V_{water}$ include uncertainty of $V_a(\text{dry})$, uncertainties of $\kappa_{sca}$ and $R_{Vf}$.

Results introduced in Sect.3.1 suggest that using the machine learning method to predict $V_a(\text{dry})$ from measurements of a three-wavelength nephelometer is feasible but non-negligible bias still exists between measured and estimated $V_a(\text{dry})$. The standard deviation of relative differences between measured and estimated $V_a(\text{dry})$ is 15%. If using triple the standard deviation (99% of points locate within this range) as the uncertainty of this method, the

Atmos. Meas. Tech. Discuss., https://doi.org/10.5194/amt-2017-330
Manuscript under review for journal Atmos. Meas. Tech.
Discussion started: 27 October 2017


uncertainty is 45%. Here, sources of this large bias is discussed. The $V_a(\text{dry})$ is determined from PNSD which is high-dimensional. Six parameters provided by the "dry" nephelometer cannot accurately constrain $R_{Vsp}$ in the machine learning method. This should be the largest uncertainty source. In addition, used datasets for training the estimator carried some uncertainties which should also influence the performance of the estimator. Using a Monte Carlo method based on uncertainties of measured PNSD (see Table 3 of Ma et al. (2014) for the uncertainty parameters of PNSD), $V_a(\text{dry})$ integrated from measured PNSD have uncertainty of about 5%. The TSI 3563 nephelometer also carry some uncertainties, it is about 9% (Heintzenberg et al., 2006;Sherman et al., 2015). Their uncertainties will propagate in the processes of training and verifying the estimator. If the datasets for training the estimator are more comprehensive (like a year of observation in several sites), the uncertainty of this machine learning method might be smaller.

The $\kappa_{sca}$ is directly fitted from $f(\text{RH})$ measurements. Results of Titos et al. (2016) demonstrate that, for moderately hygroscopic aerosols (e.g., $f(\text{RH} = 80\%)$ less than 2.2), $f(\text{RH})$ errors are around 15%. Since most values of $f(\text{RH} = 80\%)$ observed on continental regions are less than 2.2 (Zhang et al., 2015;Titos et al., 2016), 15% is used as the uncertainty of $f(\text{RH})$ as well as $\kappa_{sca}$.

As to uncertainty of estimated $R_{Vf}$. Many factors exert influences on $R_{Vf}$, such as PNSD, mixing state of BC and size-resolved $\kappa$ distribution. If using the 99% line (triple the standard deviation) shown in Fig.9b as uncertainties of $R_{Vf}$ from influences of size-resolved $\kappa$ distribution and PNSD, then this aspect of uncertainties of $R_{Vf}$ under different pollution conditions range from 17% to 49%. Additionally, the mixing state of BC can also impact on $R_{Vf}$. In this study, the

Atmos. Meas. Tech. Discuss., https://doi.org/10.5194/amt-2017-330
Manuscript under review for journal Atmos. Meas. Tech.
Discussion started: 27 October 2017

Atmospheric Measurement Techniques Discussions

BC is assumed to be half externally and half coreshell mixed with other aerosol components. A simple simulative test is performed to investigate the influence of BC mixing state on $R_{Vf}$. In this test, we simulated $R_{Vf}$ values for three kinds of BC mixing states: external; half external and half coreshell; core-shell, and the average PNSD and mass concentration of BC during Wangdu campaign are used. Simulated $R_{Vf}$ values for these three mixing state are 1.13, 1.18 and 1.25, respectively. Thus, we consider 6% as the uncertainty of $R_{Vf}$ caused by the variation of BC mixing state. The synthesized uncertainties of estimated $R_{Vf}$ under different pollution levels are presented in Fig.21, which have considered the variations of BC mixing state and size-resolved $\kappa$ distribution and PNSD. Uncertainties of estimated $R_{Vf}$ by using the look up table shown in Fig.8a range from 18% to 49.4%.

With estimated uncertainties of $V_a$(dry), $\kappa_{sca}$ and $R_{Vf}$, the uncertainties of estimated $V_{water}$ under different pollution levels can be estimated. In the processes of estimating $V_{water}$, two methods can be used to estimate $V_a$(dry). The first mehtod is estimating $V_a$(dry) from measurements of the three-wavelength "dry" nephelometer (Method 1). However, if PNSD is available, $V_a$(dry) can be directly integrated from measured PNSD (Method 2). The calculated uncertainties of $V_{water}$ under different pollution levels with $V_a$(dry) estimated from these two methods are presented in Fig.21. For Method 1, uncertainties of estimated $V_{water}$ range from 24% to 52%, with an average of 31%. For Method 2, uncertainties of estimated $V_{water}$ range from 51% to 68%%, with an average of 55%. Compared to clean conditions, the uncertainty of estimated $V_{water}$ is smaller when the air is highly polluted. We recommend that if measured PNSD is available, $V_a$(dry) should be calculated from measured PNSD, otherwise, $V_a$(dry) can be estimated from measurements of the "dry" nephelometer.

The method proposed in this research is based on datasets of PNSD, $\sigma_{sp}$ and size-resolved $\kappa$ distribution which are measured on the NCP without influences of dust and sea salt. Cautions should be exercised if using the proposed method to estimate the ALWC when the air mass is influenced by sea salt or dust. The way of estimating $V_a(\text{dry})$ with machine learning method might be applicable for different regions around the world. However, the used estimator from machine learning should be trained with corresponding regional historical datasets. The way of connecting $f(\text{RH})$ to $\text{Vg}(\text{RH})$ might also be applicable for other continental regions. Still, we suggest that the used look up table is simulated from regional historical datasets.

Note that the humidified nephelometer usually operates with RH less than 95%. Aerosol water, however, increase dramatically with increasing RH when RH is greater than 95%. Such high RH conditions can occur during the haze events. This may limits the usage of the proposed method when ambient RH is extremely high. As discussed in Sect.2.4, the proposed way of connecting $f(\text{RH})$ and $\text{Vg}(\text{RH})$ is based on the κ-K$\ddot{o}$hler theory. If κ does not change with RH, the proposed method should be applicable when RH is higher than 95%, even the measurements of humidified nephelometer system are conducted when RH is less than 95%. Many studies have done researches about the change of κ with the changing RH (Rastak et al., 2017;Renbaum-Wolff et al., 2016), their results demonstrate that the κ changes with increasing RH. However, few studies have investigated the variation of κ of ambient aerosol particles with changing RH when RH is less than 100%. Liu et al. (2011) have measured κ of ambient aerosol particles at different RHs (90%, 95%, 98.5%) on the NCP. Their results demonstrated that κ at different RHs differ little for ambient aerosol particles with different diameters. Results of Kuang et al. (2017b) indicated that κ values retrieved from $f(\text{RH})$ measurements agree well with κ values at RH of 98% of aerosol particles with diameter of 250 nm. In this respect, the proposed method might be applicable even when ambient RH is extremely high for ambient aerosol particles on the NCP. Moreover, for calculating the ambient ALWC, the measured ambient RH is required. However, if the ambient RH is higher than 95%, the measured ambient RH with current techniques is highly uncertain. Given this, cautions should be exercised if the ambient ALWC is calculated when the ambient RH is higher than 95%.

## 4. conclusions

In this paper, a novel method is proposed to calculate ALWC based on measurements of a three-wavelength humidified nephelometer system. Two critical relationships are required in this method. One is the relationship between $V_a$(dry) and measurements of the "dry" nephelometer. Another one is the relationship between Vg(RH) and $f$(RH). The ALWC can be calculated from the estimated $V_a$(dry) and Vg(RH).

Previous studies have shown that an approximate proportional relationship exists between $V_a$(dry) and corresponding $\sigma_{sp}$, especially for fine particles (particle diameter less than 1 μm). However, PNSD and other factors still have significant influences on this proportional relationship. It is difficult to directly estimate $V_a$(dry) from measured $\sigma_{sp}$. In this paper, an estimator from machine learning procedure is used to estimate $V_a$(dry) based on measurements of a three-wavelength nephelometer. This estimator is trained with datasets of PNSD and $\sigma_{sp}$ from several field campaigns conducted on the NCP. This method is then validated using measurements from Wangdu campaign. The square of correlation coefficient between measured and estimated $V_a$(dry) is 0.93.

Atmos. Meas. Tech. Discuss., https://doi.org/10.5194/amt-2017-330
Manuscript under review for journal Atmos. Meas. Tech.
Discussion started: 27 October 2017




The relationship between Vg(RH) and $f$(RH) is then investigated by conducting a simulative experiment. It is found that the complicated relationship between Vg(RH) and $f$(RH) can be disentangled by using a look up table, and parameters required in the look up table can be directly calculated from measurements of a three-wavelength humidified nephelometer system. Given that the $V_a$(dry) can be estimated from a three-wavelength "dry" nephelometer, the ambient ALWC can be estimated from measurements of a three-wavelength humidified nephelometer system in conjunction with measured ambient RH. During Wangdu campaign, calculated water volumes of ambient aerosol particles range from 1 to 300 $\mu m^3/cm^3$, with an average of 42 $\mu m^3/cm^3$.

Results introduced in this research have bridged the gap between $f$(RH) and Vg(RH). The advantage of using measurements of a humidified nephelometer system to estimate ALWC is that this technique has a fast response time and can provide continuous measurements of the changing ambient conditions. The new method proposed in this research will facilitate the real-time monitoring of the ambient ALWC and further our understanding of roles of ALWC in atmospheric chemistry, secondary aerosol formation and climate change.

## Acknowledgments

This work is supported by the National Natural Science Foundation of China (41590872, 41375134). The data used are listed in the references and a repository at http://pan.baidu.com/s/1c2Nzc5a.

## References

Anderson, T., Covert, D., Marshall, S., Laucks, M., Charlson, R., Waggoner, A., Ogren, J., Caldow, R., Holm, R., and Quant, F.: Performance characteristics of a high-sensitivity, three-wavelength, total scatter/backscatter nephelometer, Journal of Atmospheric and Oceanic Technology, 13, 967-986, 1996.

Atmos. Meas. Tech. Discuss., https://doi.org/10.5194/amt-2017-330
Manuscript under review for journal Atmos. Meas. Tech.
Discussion started: 27 October 2017


Anderson, T. L., and Ogren, J. A.: Determining aerosol radiative properties using the TSI 3563 integrating nephelometer, Aerosol Science and Technology, 29, 57-69, 10.1080/02786829808965551, 1998.

Bian, Y. X., Zhao, C. S., Ma, N., Chen, J., and Xu, W. Y.: A study of aerosol liquid water content based on hygroscopicity measurements at high relative humidity in the North China Plain, Atmos. Chem. Phys., 14, 6417-6426, 10.5194/acp-14-6417-2014, 2014.

Birmili, W., Stratmann, F., and Wiedensohler, A.: Design of a DMA-based size spectrometer for a large particle size range and stable operation, Journal of Aerosol Science, 30, 549-553, 10.1016/s0021-8502(98)00047-0, 1999.

Bohren, C. F., and Huffman, D. R.: Absorption and scattering of light by small particles, Wiley, New York, USA, 2008.

Brock, C. A., Wagner, N. L., Anderson, B. E., Attwood, A. R., Beyersdorf, A., Campuzano-Jost, P., Carlton, A. G., Day, D. A., Diskin, G. S., Gordon, T. D., Jimenez, J. L., Lack, D. A., Liao, J., Markovic, M. Z., Middlebrook, A. M., Ng, N. L., Perring, A. E., Richardson, M. S., Schwarz, J. P., Washenfelder, R. A., Welti, A., Xu, L., Ziemba, L. D., and Murphy, D. M.: Aerosol optical properties in the southeastern United States in summer – Part 1: Hygroscopic growth, Atmos. Chem. Phys., 16, 4987-5007, 10.5194/acp-16-4987-2016, 2016.

Cheng, Y., Zheng, G., Wei, C., Mu, Q., Zheng, B., Wang, Z., Gao, M., Zhang, Q., He, K., Carmichael, G., Pöschl, U., and Su, H.: Reactive nitrogen chemistry in aerosol water as a source of sulfate during haze events in China, Science Advances, 2, 10.1126/sciadv.1601530, 2016.

Covert, D. S., Charlson, R., and Ahlquist, N.: A study of the relationship of chemical composition and humidity to light scattering by aerosols, Journal of applied meteorology, 11, 968-976, 1972.

Engelhart, G. J., Hildebrandt, L., Kostenidou, E., Mihalopoulos, N., Donahue, N. M., and Pandis, S. N.: Water content of aged aerosol, Atmos. Chem. Phys., 11, 911-920, 10.5194/acp-11-911-2011, 2011.

Fierz-Schmidhauser, R., Zieger, P., Vaishya, A., Monahan, C., Bialek, J., O'Dowd, C. D., Jennings, S. G., Baltensperger, U., and Weingartner, E.: Light scattering enhancement factors in the marine boundary layer (Mace Head, Ireland), Journal of Geophysical Research: Atmospheres, 115, D20204, 10.1029/2009JD013755, 2010.

Hegg, D., Larson, T., and Yuen, P.-F.: A theoretical study of the effect of relative humidity on light scattering by tropospheric aerosols, Journal of Geophysical Research: Atmospheres, 98, 18435-18439, 10.1029/93JD01928, 1993.

Heintzenberg, J., Wiedensohler, A., Tuch, T. M., Covert, D. S., Sheridan, P., Ogren, J. A., Gras, J., Nessler, R., Kleefeld, C., Kalivitis, N., Aaltonen, V., Wilhelm, R. T., and Havlicek, M.: Intercomparisons and Aerosol Calibrations of 12 Commercial Integrating Nephelometers of Three Manufacturers, Journal of Atmospheric and Oceanic Technology, 23, 902-914, 10.1175/JTECH1892.1, 2006.

Kuang, Y., Zhao, C. S., Tao, J. C., and Ma, N.: Diurnal variations of aerosol optical properties in the North China Plain and their influences on the estimates of direct aerosol radiative effect, Atmos. Chem. Phys., 15, 5761-5772, 10.5194/acp-15-5761-2015, 2015.

Kuang, Y., Zhao, C. S., Tao, J. C., Bian, Y. X., and Ma, N.: Impact of aerosol hygroscopic growth on the direct aerosol radiative effect in summer on North China Plain, Atmospheric Environment, 147, 224-233, http://dx.doi.org/10.1016/j.atmosenv.2016.10.013, 2016.

Kuang, Y., Zhao, C., Tao, J., Bian, Y., Ma, N., and Zhao, G.: A novel method to derive the aerosol hygroscopicity parameter based only on measurements from a humidified nephelometer system, Atmos. Chem. Phys. Discuss., 2017, 1-25, 10.5194/acp-2016-1066, 2017a.

Kuang, Y., Zhao, C., Tao, J., Bian, Y., Ma, N., and Zhao, G.: A novel method for deriving the aerosol hygroscopicity parameter based only on measurements from a humidified nephelometer system, Atmos. Chem. Phys., 17, 6651-6662, 10.5194/acp-17-6651-2017, 2017b.
Liu, H. J., Zhao, C. S., Nekat, B., Ma, N., Wiedensohler, A., van Pinxteren, D., Spindler, G., Müller, K., and Herrmann, H.: Aerosol hygroscopicity derived from size-segregated chemical composition and its parameterization in the North China Plain, Atmos. Chem. Phys., 14, 2525-2539, 10.5194/acp-14-2525-2014, 2014.
Liu, P. F., Zhao, C. S., Göbel, T., Hallbauer, E., Nowak, A., Ran, L., Xu, W. Y., Deng, Z. Z., Ma, N., Mildenberger, K., Henning, S., Stratmann, F., and Wiedensohler, A.: Hygroscopic properties of aerosol particles at high relative humidity and their diurnal variations in the North China Plain, Atmos. Chem. Phys., 11, 3479-3494, 10.5194/acp-11-3479-2011, 2011.
Ma, N., Zhao, C. S., Müller, T., Cheng, Y. F., Liu, P. F., Deng, Z. Z., Xu, W. Y., Ran, L., Nekat, B., van Pinxteren, D., Gnauk, T., Müller, K., Herrmann, H., Yan, P., Zhou, X. J., and Wiedensohler, A.: A new method to determine the mixing state of light absorbing carbonaceous using the measured aerosol optical properties and number size distributions, Atmos. Chem. Phys., 12, 2381-2397, 10.5194/acp-12-2381-2012, 2012.
Ma, N., Birmili, W., Müller, T., Tuch, T., Cheng, Y. F., Xu, W. Y., Zhao, C. S., and Wiedensohler, A.: Tropospheric aerosol scattering and absorption over central Europe: a closure study for the dry particle state, Atmos. Chem. Phys., 14, 6241-6259, 10.5194/acp-14-6241-2014, 2014.
Martin, S. T.: Phase Transitions of Aqueous Atmospheric Particles, Chem. Rev., 100, 3403-3454, 10.1021/cr990034t, 2000.
Meier, J., Wehner, B., Massling, A., Birmili, W., Nowak, A., Gnauk, T., Brüggemann, E., Herrmann, H., Min, H., and Wiedensohler, A.: Hygroscopic growth of urban aerosol particles in Beijing (China) during wintertime: a comparison of three experimental methods, Atmos. Chem. Phys., 9, 6865-6880, 10.5194/acp-9-6865-2009, 2009.
Pedregosa, F., Varoquaux, G., Gramfort, A., Michel, V., Thirion, B., Grisel, O., Blondel, M., Prettenhofer, P., Weiss, R., Dubourg, V., Vanderplas, J., Passos, A., Cournapeau, D., Brucher, M., Perrot, M., and Duchesnay, E.: Scikit-learn: Machine Learning in Python, Journal of Machine Learning Research, 12, 2825-2830, 2011.
Petters, M. D., and Kreidenweis, S. M.: A single parameter representation of hygroscopic growth and cloud condensation nucleus activity, Atmospheric Chemistry and Physics, 7, 1961-1971, 2007.
Pinnick, R. G., Jennings, S. G., and Chýlek, P.: Relationships between extinction, absorption, backscattering, and mass content of sulfuric acid aerosols, Journal of Geophysical Research: Oceans, 85, 4059-4066, 10.1029/JC085iC07p04059, 1980.
Rader, D. J., and McMurry, P. H.: Application of the tandem differential mobility analyzer to studies of droplet growth or evaporation, Journal of Aerosol Science, 17, 771-787, http://dx.doi.org/10.1016/0021-8502(86)90031-5, 1986.
Rastak, N., Pajunoja, A., Acosta Navarro, J. C., Ma, J., Song, M., Partridge, D. G., Kirkevåg, A., Leong, Y., Hu, W. W., Taylor, N. F., Lambe, A., Cerully, K., Bougiatioti, A., Liu, P., Krejci, R., Petäjä, T., Percival, C., Davidovits, P., Worsnop, D. R., Ekman, A. M. L., Nenes, A., Martin, S., Jimenez, J. L., Collins, D. R., Topping, D. O., Bertram, A. K., Zuend, A., Virtanen, A., and Riipinen, I.: Microphysical explanation of the RH-dependent water affinity of biogenic organic aerosol and its importance for climate, Geophys. Res. Lett., 44, 5167-5177, 10.1002/2017GL073056, 2017.
Renbaum-Wolff, L., Song, M., Marcolli, C., Zhang, Y., Liu, P. F., Grayson, J. W., Geiger, F. M., Martin, S. T., and Bertram, A. K.: Observations and implications of liquid–liquid phase separation at high relative humidities in secondary organic material produced by α-pinene ozonolysis without

Atmos. Meas. Tech. Discuss., https://doi.org/10.5194/amt-2017-330
Manuscript under review for journal Atmos. Meas. Tech.
Discussion started: 27 October 2017

Atmospheric Measurement Techniques Discussions

inorganic salts, Atmos. Chem. Phys., 16, 7969-7979, 10.5194/acp-16-7969-2016, 2016.

Seinfeld, J. H., and Pandis, S. N.: Atmospheric chemistry and physics: from air pollution to climate change, John Wiley & Sons, 2006.

Sherman, J. P., Sheridan, P. J., Ogren, J. A., Andrews, E., Hageman, D., Schmeisser, L., Jefferson, A., and Sharma, S.: A multi-year study of lower tropospheric aerosol variability and systematic relationships from four North American regions, Atmos. Chem. Phys., 15, 12487-12517, 10.5194/acp-15-12487-2015, 2015.

Tao, J. C., Zhao, C. S., Ma, N., and Liu, P. F.: The impact of aerosol hygroscopic growth on the single-scattering albedo and its application on the NO2 photolysis rate coefficient, Atmos. Chem. Phys., 14, 12055-12067, 10.5194/acp-14-12055-2014, 2014.

Titos, G., Cazorla, A., Zieger, P., Andrews, E., Lyamani, H., Granados-Muñoz, M. J., Olmo, F. J., and Alados-Arboledas, L.: Effect of hygroscopic growth on the aerosol light-scattering coefficient: A review of measurements, techniques and error sources, Atmospheric Environment, 141, 494-507, http://dx.doi.org/10.1016/j.atmosenv.2016.07.021, 2016.

Wang, G., Zhang, R., Gomez, M. E., Yang, L., Levy Zamora, M., Hu, M., Lin, Y., Peng, J., Guo, S., Meng, J., Li, J., Cheng, C., Hu, T., Ren, Y., Wang, Y., Gao, J., Cao, J., An, Z., Zhou, W., Li, G., Wang, J., Tian, P., Marrero-Ortiz, W., Secrest, J., Du, Z., Zheng, J., Shang, D., Zeng, L., Shao, M., Wang, W., Huang, Y., Wang, Y., Zhu, Y., Li, Y., Hu, J., Pan, B., Cai, L., Cheng, Y., Ji, Y., Zhang, F., Rosenfeld, D., Liss, P. S., Duce, R. A., Kolb, C. E., and Molina, M. J.: Persistent sulfate formation from London Fog to Chinese haze, Proc Natl Acad Sci U S A, 10.1073/pnas.1616540113, 2016.

Wex, H., Neususs, C., Wendisch, M., Stratmann, F., Koziar, C., Keil, A., Wiedensohler, A., and Ebert, M.: Particle scattering, backscattering, and absorption coefficients: An in situ closure and sensitivity study, Journal of Geophysical Research-Atmospheres, 107, 18, 10.1029/2000jd000234, 2002.

Wiedensohler, A., Birmili, W., Nowak, A., Sonntag, A., Weinhold, K., Merkel, M., Wehner, B., Tuch, T., Pfeifer, S., Fiebig, M., Fjäraa, A. M., Asmi, E., Sellegri, K., Depuy, R., Venzac, H., Villani, P., Laj, P., Aalto, P., Ogren, J. A., Swietlicki, E., Williams, P., Roldin, P., Quincey, P., Hüglin, C., Fierz-Schmidhauser, R., Gysel, M., Weingartner, E., Riccobono, F., Santos, S., Grüning, C., Faloon, K., Beddows, D., Harrison, R., Monahan, C., Jennings, S. G., O'Dowd, C. D., Marinoni, A., Horn, H. G., Keck, L., Jiang, J., Scheckman, J., McMurry, P. H., Deng, Z., Zhao, C. S., Moerman, M., Henzing, B., de Leeuw, G., Löschau, G., and Bastian, S.: Mobility particle size spectrometers: harmonization of technical standards and data structure to facilitate high quality long-term observations of atmospheric particle number size distributions, Atmos. Meas. Tech., 5, 657-685, 10.5194/amt-5-657-2012, 2012.

Wu, Z. J., Zheng, J., Shang, D. J., Du, Z. F., Wu, Y. S., Zeng, L. M., Wiedensohler, A., and Hu, M.: Particle hygroscopicity and its link to chemical composition in the urban atmosphere of Beijing, China, during summertime, Atmos. Chem. Phys., 16, 1123-1138, 10.5194/acp-16-1123-2016, 2016.

Zhang, L., Sun, J. Y., Shen, X. J., Zhang, Y. M., Che, H., Ma, Q. L., Zhang, Y. W., Zhang, X. Y., and Ogren, J. A.: Observations of relative humidity effects on aerosol light scattering in the Yangtze River Delta of China, Atmos. Chem. Phys., 15, 8439-8454, 10.5194/acp-15-8439-2015, 2015.

Zieger, P., Fierz-Schmidhauser, R., Gysel, M., Ström, J., Henne, S., Yttri, K. E., Baltensperger, U., and Weingartner, E.: Effects of relative humidity on aerosol light scattering in the Arctic, Atmos. Chem. Phys., 10, 3875-3890, 10.5194/acp-10-3875-2010, 2010.

Table 1 Abbreviations

| | |
|---|---|
| RH | relative humidity |
| $f$(RH) | aerosol light scattering enhancement factor at 550 nm |
| ALWC | aerosol liquid water content |
| $V_a$(dry) | total volume of ambient aerosol particles in dry state |
| Vg(RH) | aerosol volume enhancement factor due to water uptake |
| NCP | North China Plain |
| HTDMA | humidified tandem differential mobility analyser system |
| PNSD | particle number size distribution |
| BC | black carbon |
| g(RH) | hygroscopic growth factor |
| APS | Aerodynamic Particle Sizer |
| SMPS | scanning mobility particle size spectrometer |
| $\sigma_{sp}$ | aerosol light scattering coefficient |
| $\sigma_{bsp}$ | aerosol back scattering coefficient |
| $\sigma_{ext}$ | aerosol extinction coefficient |
| $R_{Vsp}$ | $\sigma_{sp}(550\ nm)/V_a$(dry) |
| F1 to F5 | referred as to five field campaigns listed in Table S1 |
| D1 | PNSD, BC and nephelometer measurements from field campaigns F1 to F4 |
| D2 | PNSD, BC and nephelometer measurements from F2, F4 and F5 |

Atmos. Meas. Tech. Discuss., https://doi.org/10.5194/amt-2017-330
Manuscript under review for journal Atmos. Meas. Tech.
Discussion started: 27 October 2017


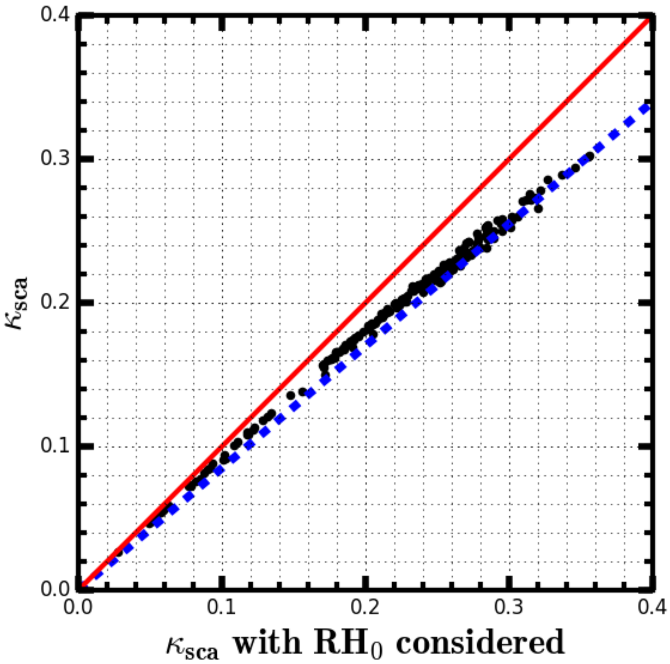


**Figure 1**. X-axis and y-axis represent $\kappa_{sca}$ are fitted with and without consideration of $RH_0$ in the “dry” nephelometer, respectively. The red line is 1:1 line, the blue dashed line is the 15% relative difference line.

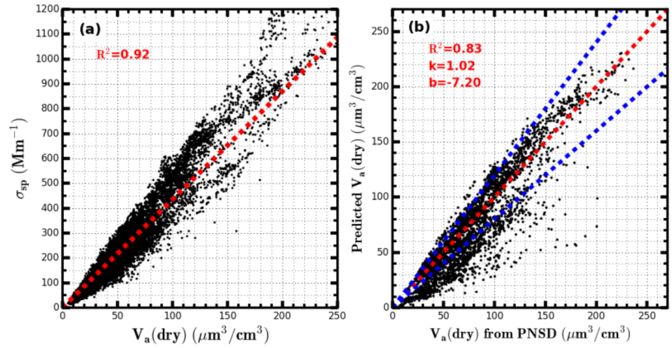


**Figure 2**. (a) Scatter plot of all valid data points of $V_a$(dry) and $\sigma_{sp}$ at 550 nm from D1, dashed red line is the line whose slope is equal to the average ratio $\sigma_{sp}(550\ nm)/V_a(\text{dry})(R_{Vsp})$. (b) The comparison between $V_a$(dry) estimated from a fixed average $R_{Vsp}$ of (a) and measured $V_a$(dry). In figure (a), the dashed red line is the line whose slope is the average ratio $R_{Vsp}$. In figure (b), red line is the 1:1 line, two dashed blue line are lines with relative difference of 20%. $R^2$ is the suqare of correlation coefficient, k is the slope, b is the intercept.

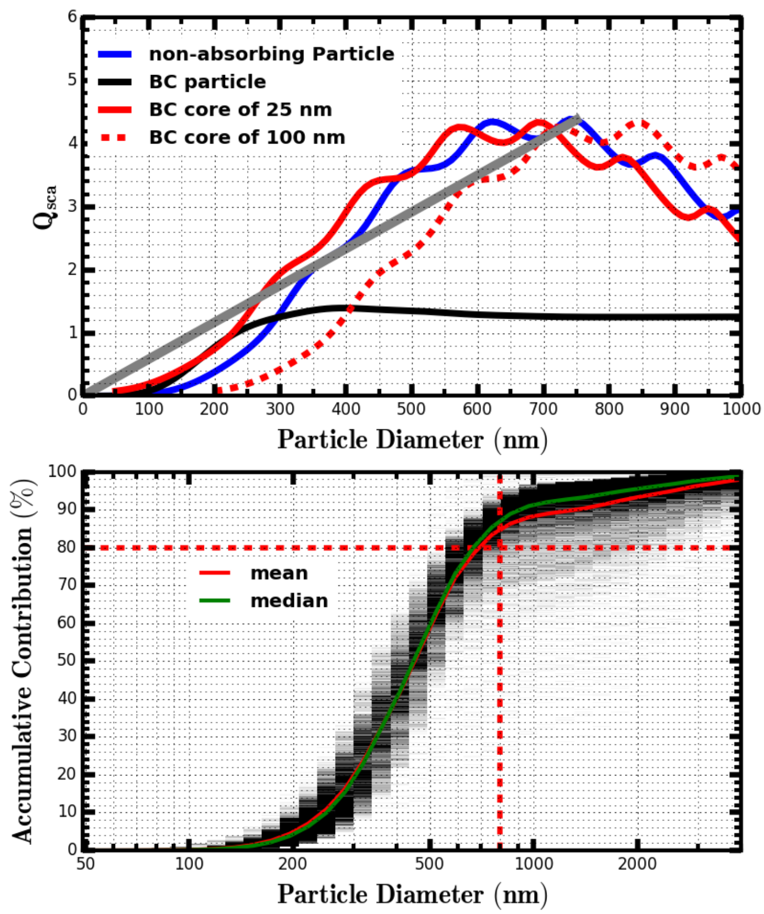


**Figure 3**. (a) $Q_{sca}$ at 550 nm as a function of particle diameter for four types of aerosol particles, the gray line corresponds to the fitted linear line for the case of non-absorbing particle when particle diameter is less than 750 nm. (b) Simulated size-resolved accumulative contribution to scattering coefficient at 550 nm for all PNSDs measured during Wangdu campaign, the color scales (from light gray to black) represent occurrences.

Atmos. Meas. Tech. Discuss., https://doi.org/10.5194/amt-2017-330
Manuscript under review for journal Atmos. Meas. Tech.
Discussion started: 27 October 2017


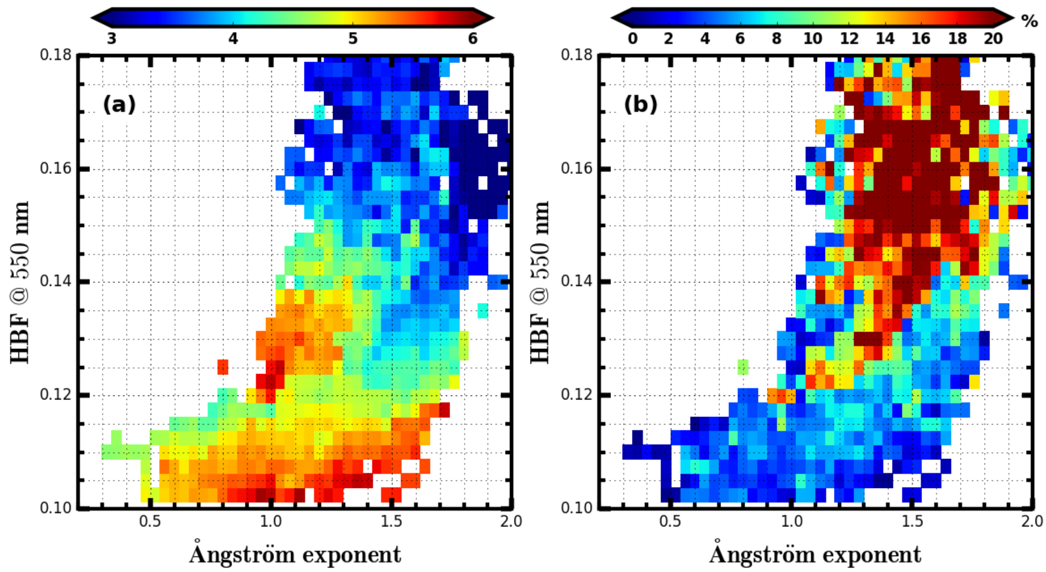


**Figure 4**. (a) Colors represent $R_{Vsp}$ values and the color bar is shown on the top of this figure, x-axis represents Ångström exponent and y-axis represents HBF at 550 nm. (b) Meanings of x-axis and y-axis are same with them in (a), however, color represents the percentile value of the standard deviation of $R_{Vsp}$ values within each grid divided by their average.

718 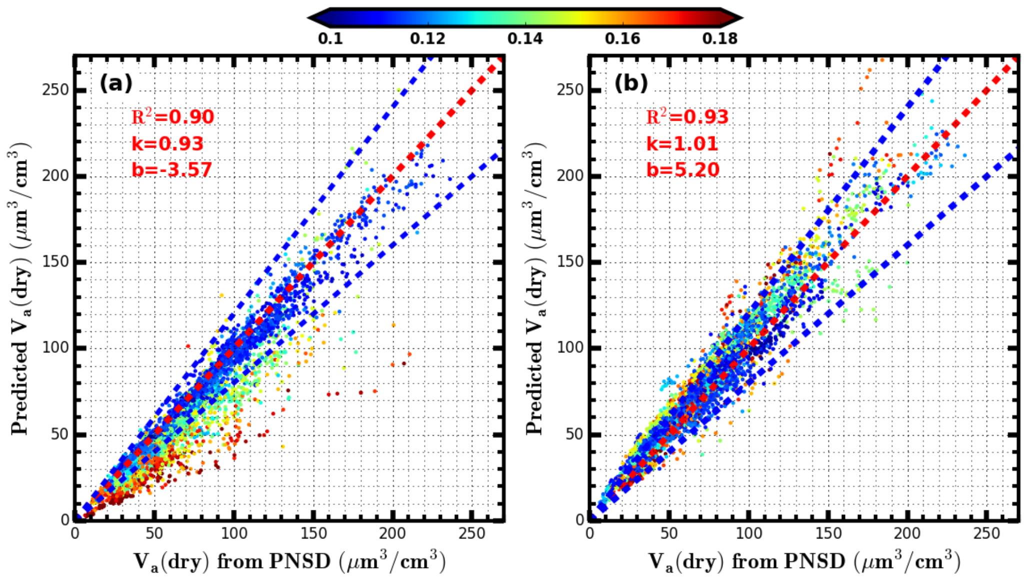


719 **Figure 5**. Comparisons between predicted and measured $V_a$(dry), the red dashed line is the 1:1 line, two blue
720 dashed line shown in (a) and (b) are lines with relative difference of 20%. Colors of scattered points in (a) and
721 (b) represent corresponding values of HBF at 550 nm, and the color bar is shown on the top. (a) $V_a$(dry) in the
722 y-axis is predicted by using results shown in Fig.4a as a look up table. (b) $V_a$(dry) in the y-axis is predicted by
723 using the machine learning method.
724

Atmos. Meas. Tech. Discuss., https://doi.org/10.5194/amt-2017-330
Manuscript under review for journal Atmos. Meas. Tech.
Discussion started: 27 October 2017


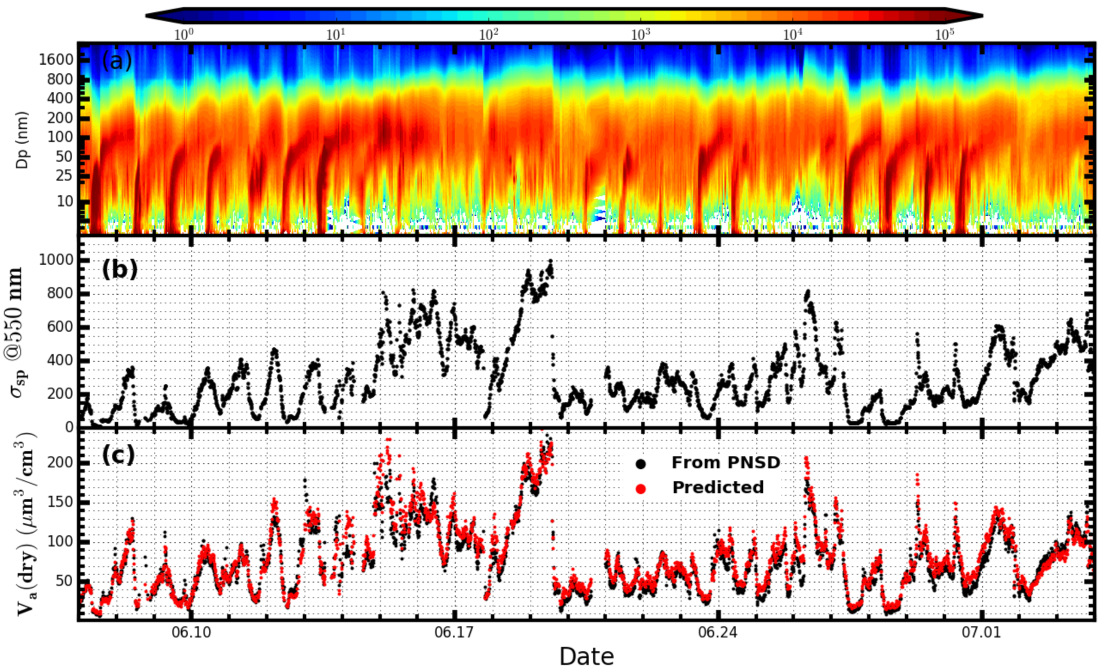


**Figure 6**. Measurements of PNSD and $\sigma_{sp}$ during Wangdu campaign; (a) Time series of PNSD in dry state, colors represent $dN/dlog(Dp)(cm^{-3})$; (b) Time series of measured $\sigma_{sp}$ at 550 nm; (c) $V_a$(dry) integrated from measured PNSD and $V_a$(dry) predicted by using the machine learning method.

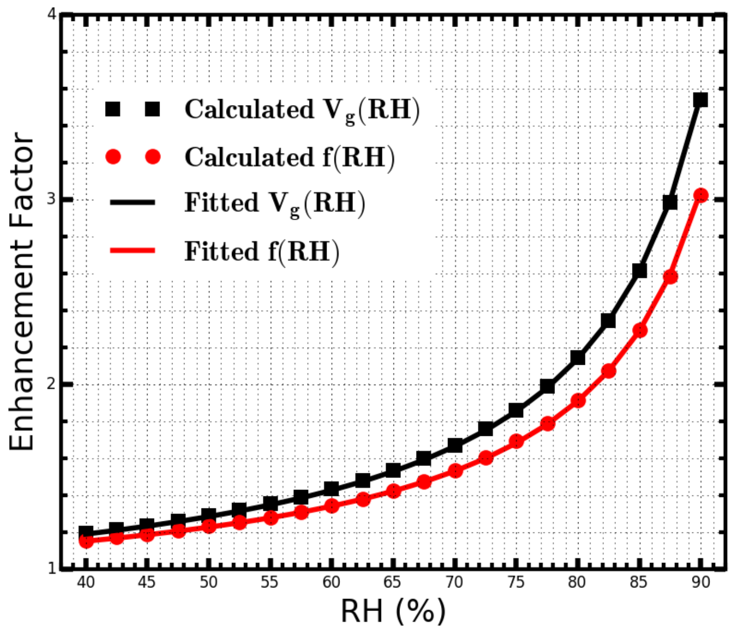


**Figure 7**. Modelled $f$(RH) and Vg(RH) (scatter points) and fitted $f$(RH) and Vg(RH) (solid lines) using formula form of equation (2).

Atmos. Meas. Tech. Discuss., https://doi.org/10.5194/amt-2017-330
Manuscript under review for journal Atmos. Meas. Tech.
Discussion started: 27 October 2017


Atmospheric Measurement Techniques
Open Access
Discussions

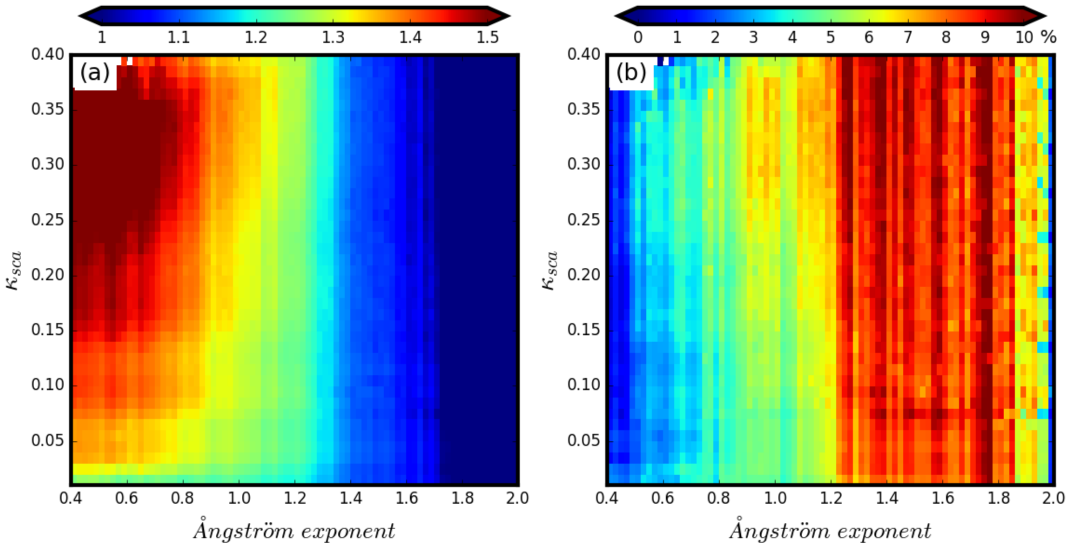


**Figure 8**. (a) Colors represent $R_{Vf}$ values and the colorbar is shown on the top of this figure, x-axis represents Ångström exponent and y-axis represents $\kappa_{sca}$. (b) Meanings of x-axis and y-axis are same with them in (a), however, color represents the percentile value of the standard deviation of $R_{Vf}$ values within each grid divided by their average.

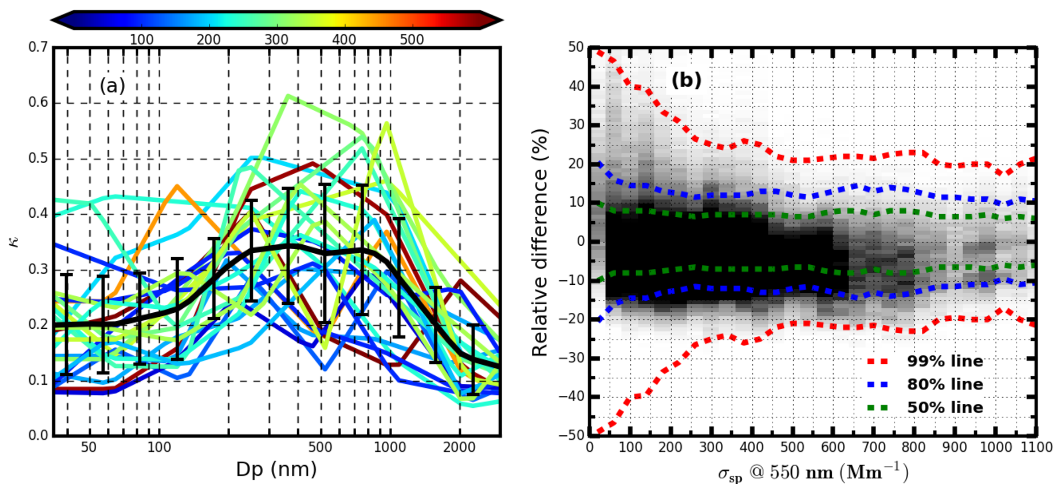


**Figure 9**. (a) All size-resolved $\kappa$ distributions which are derived from measured size-segregated chemical compositions during HaChi campaign, colors represent corresponding values of average $\sigma_{sp}$ at 550 nm ($Mm^{-1}$), black solid line is the average size-resolved $\kappa$ distribution and error bars are standard deviations ; (b) The gray

Atmos. Meas. Tech. Discuss., https://doi.org/10.5194/amt-2017-330
Manuscript under review for journal Atmos. Meas. Tech.
Discussion started: 27 October 2017


Atmospheric Measurement Techniques
Discussions

colors represent the distribution of relative differences between modelled and estimated $R_{Vf}$ values, darker grids have higher frequency, dashed lines with the same color mean that corresponding percentile of points locate between the two lines.

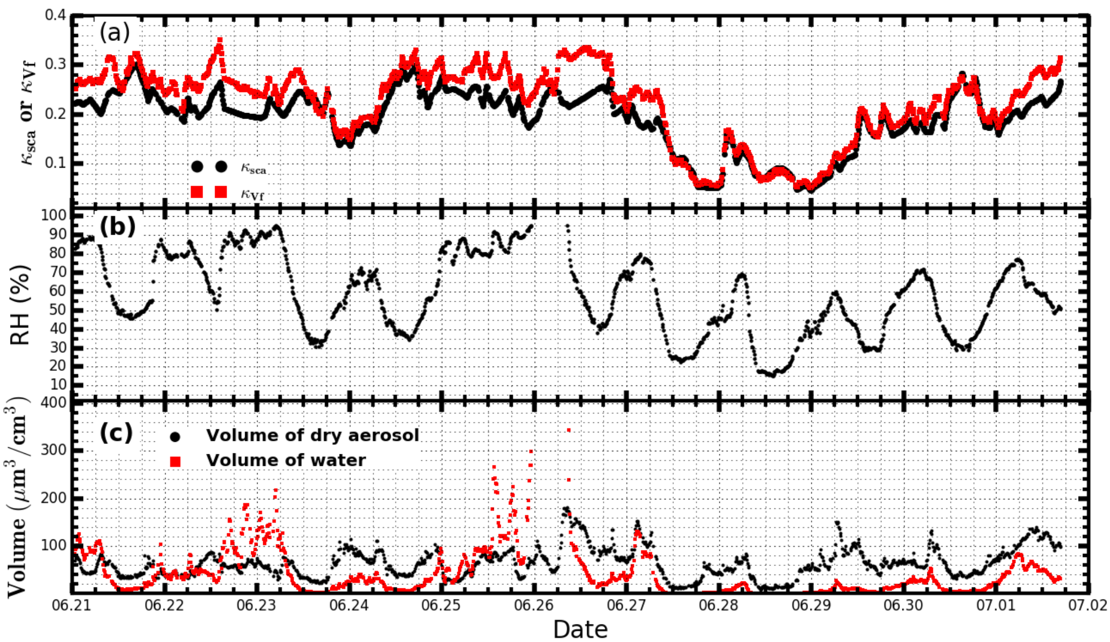


**Figure 10.** (a) Time series of values of $\kappa_{sca}$ fitted from observed $f$(RH) curves and predicted values of $\kappa_{Vf}$ by using results shown in Fig.8a as a look up table; (b) Measured amibient RH; (c) Time series of $V_a$(dry) ($\mu m^3/cm^3$) which is integrated from measured PNSD and volume of aerosol liquid water estimated from combination of $\kappa_{Vf}$ and ambient RH.

Atmospheric Measurement Techniques
Open Access
Discussions

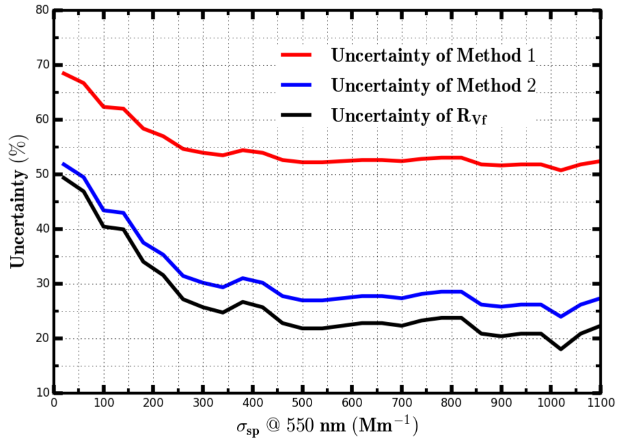


**Figure 11**. Black line corresponds to uncertainty of predicted $R_{Vf}$ by using results shown in Fig.5a as the look up table. Blue and red lines represent uncertainties of volumes of aerosol liquid water which are estimated from the following two methods: Method 1 corresponds to $V_a$(dry) is estimated from the machine learning method, Method 2 corresponds to $V_a$(dry) is integrated from the concurrently measured PNSD.